LASER INTERFEROMETER GRAVITATIONAL WAVE OBSERVATORY

– LIGO –

CALIFORNIA INSTITUTE OF TECHNOLOGY

MASSACHUSETTS INSTITUTE OF TECHNOLOGY

Document Type	**LIGO-T010159-00-R**	**10/15/01**

The Pre Stabilized Laser for the LIGO Caltech 40m Interferometer: Stability Controls and Characterization.

Andrea De Michele, Alan Weinstein, Dennis Ugolini

Distribution of this draft:

This is an internal working note
Of the LIGO Project

California Institute of Technology
LIGO Project – MS 51-33
Pasadena, CA 91125
Phone (626)395-2129
Fax (626)304-9834
E-mail: info@ligo.caltech.edu

Massachusetts Institute of Technology
LIGO Project – MS 20B-145
Cambridge, MA 01239
Phone (617)253-4824
Fax (617)253-7014
E-mail: info@ligo.mit.edu

WWW: http://www.ligo.caltech.edu

The Pre Stabilized Laser for the LIGO Caltech 40m Interferometer: Stability Controls and Characterization.

Abstract

The purpose of this work is the characterization of the control loops in the Pre-Stabilized laser (PSL), recently installed in LIGO 40m interferometer in Caltech. The 40m interferometer is a prototype of the real LIGO interferometer used to detect gravitational waves. In order to minimize the noise of the PSL there are several Stability Control Systems. In this work I test these Stability Controls and I measure the noise of the laser when these controls are engaged. I measure the frequency noise of the laser, the position and angle fluctuations of the beam, and I test the frequency servo system and the Pre-mode cleaner servo. I study the frequency spectrum of the noise up to 1 kHz and the long term-fluctuations over several days.

Andrea De Michele
Mentor: Alan J. Weinstein, Dennis Ugolini
August 24, 2001

Contents

1 LIGO.

LIGO (Laser Interferometer Gravitational-wave Observatory) is an observatory to detect gravitational waves.[1] It is based on a Michelson interferometer with the mirrors (test masses) free to move. The Michelson interferometer is a precise instrument for measuring the position of test masses that depend on interaction with gravitational waves. To detect the gravitational waves the Michelson interferometer must have an optical length about 1000 km and this is obtained with folded interferometer arms with physical length about 4 km. There are two 4 km LIGO interferometers, one at Hanford and one at Livingston, and one 2 km interferometer at Hanford.

At Caltech there is a small prototype (**IFO**), 40 m long, to test the performance and the noise of this kind of interferometer.

The source of light of the interferometer is a laser. The purpose of this work is test the servo control system of the laser and measure the noise of the laser.

2 Pre-Stabilized Laser and LIGO Performance.

PSL, Pre-Stabilized Laser, is the source of light of the interferometer (**IFO**).[2] [3] It includes the laser and all the optical and electro-optical devices to make frequency, amplitude and mode stabilization.

To measure the test mass displacement we measure the phase shift between the two beams in the two different arms. According to the interference laws the power of the output of the IFO is correlated with the phase shift between the two arms as follow:

$$P_{out} = P_{in} \cdot \cos^2(\phi). \tag{1}$$

Where P_{in} is the laser's power, $\phi = 2 \cdot k \cdot \Delta L$ is the phase shift. k is the wavenumber ($k = 2\pi/\lambda$) and ΔL is the length difference between the two arms. In this way we measure a light power to measure the mirror's displacement. If we have noise in the laser, we have noise in our displacement measurement.

2.1 Readout noise: shot noise and pressure noise.

The readout noise is one of the fundamental noises of LIGO, and it is the only fundamental noise due to the laser.

Figure 1 shows the LIGO fundamental noise sources. The readout noise of the laser is the *shot noise* plus the *pressure noise*.

The shot noise has its origin in the particle nature of light (photon). To measure the power of light is the same thing to count the number of photons in a time unit. The counting of discrete independent events follows the *Poisson statistic*. If we count the number of photon N in the time interval τ the fractional precision is:

$$\frac{\sigma_{\overline{N}}}{\overline{N}} = \frac{1}{\sqrt{\overline{n}\tau}}. \tag{2}$$

Where $\overline{n}$ is the mean number of photon in the time unit.

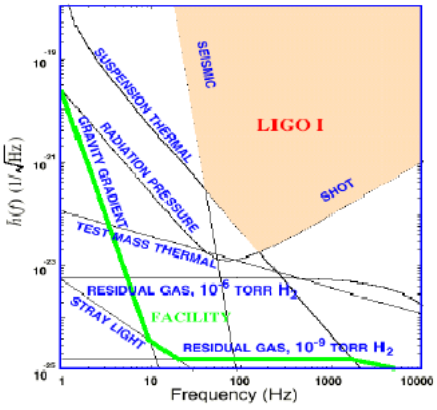

Figure 1: LIGO fundamental noise.

Thus the shot noise on the length of the arm is:

$$h_{sh}(f) = \frac{\delta L}{L} = \frac{1}{L} \cdot \sqrt{\frac{\hbar c \lambda}{2\pi T(f) P_{in}}}. \tag{3}$$

Where P_{in} is the power of laser, L is the length of the interferometer and $T(f) = d(P_{out}/P_{in})/d\phi$ is the unitless transfer function of the IFO.

We can see that if the power of laser increases the noise decreases, and if the wavelength decreases also the noise increases. Using a high power laser we can minimize the shot noise. The choice of wavelength cannot be arbitrary because there are not high power laser devices available at all wavelengths. Nd:YAG lasers, with wavelength = 1064 nm, are an industry-standard laser technology, capable of producing CW power of 10's or even 100's of watts; this is the laser technology chosen for LIGO.

The pressure noise is due to the force of the light on the mirrors:

$$h_{rp}(f) = \frac{\delta L}{L} = \frac{2}{mf^2} \cdot \sqrt{\frac{\hbar T(f) P_{in}}{8\pi^3 c \lambda}}. \tag{4}$$

This kind of noise increases when the power of the laser increases, and it is high at low frequency.

Because the shot noise and the pressure noise are not correlated in initial LIGO, the readout noise is:

$$h_{ro} = \sqrt{h_{sh}^2 + h_{rp}^2}. \tag{5}$$

It is necessary choose the right power of the laser to put the minimum of h_{ro} in the frequency that we want.

2.2 Other noise sources.

There are many other noise sources from the laser. These include:

- frequency noise
- intensity noise
- pointing and angle fluctuations

All these propagate to the IFO output. It is necessary to minimize them in the way that they are lower than the fundamental noises. The frequency noise changes the phase of Equation 1 because the Michelson dark port condition (contrast) is not perfect, so that noise common to both arms do not perfectly cancel at the beam splitter. The intensity noise changes the P_{in} of Equation 1. The pointing and angle fluctuations change the optic length of the arms (the length of the light path).

The PSL design has the purpose of minimize these noise sources with different techniques, to prepare the light for the IFO.

3 PSL: Operating Principles.

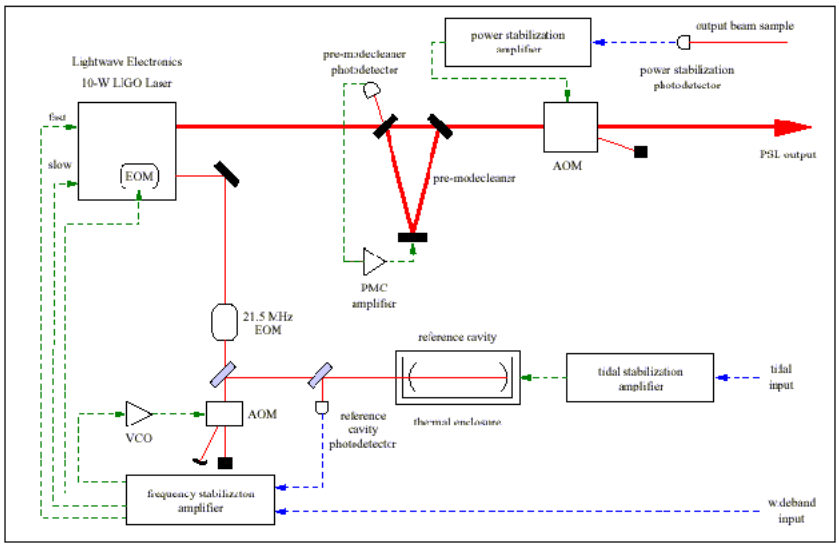

Figure 2: PSL layout.

Figure 2 represents the PSL layout. The laser is the box on the left upper corner. It has two output beams, one of high power, and one of low power. The low power beam is used for the Frequency Stabilization Servo-System(**FSS**). The

frequency of the laser is compared with the resonant frequency of a reference cavity, and the error signal obtained is sent in feedback to the laser for frequency stabilization and to minimize the frequency noise. The high power beam is sent to the IFO, after it resonates in the Pre-Mode Cleaner Cavity (**PMC**). After the PMC the transverse profile of the beam is a near-perfect TEM_{00} Gaussian mode, and the intensity noise is reduced. In this beam there is also the Intensity Servo-System (**ISS**) with the goal to reduce the intensity noise.

3.1 Lightwave MOPA laser

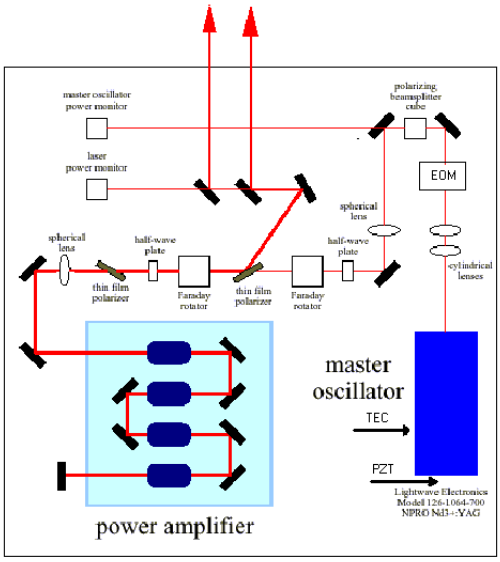

Figure 3: MOPA.

The laser is the *126 MOPA Laser*. It was designed and developed by Lightwave Electronics Inc., Mountain View, CA (in collaboration with LIGO physicists). It is a Master-Oscillator-Power-Amplifier (**MOPA**) based on a diode-pumped, narrow-linewidth, single frequency laser as the master oscillator and a double-passed power amplifier. Figure 3 shows the laser layout. Some specifications of the laser are:

- High power beam: 10 W
- Low power beam: 10 mW
- Wavelength: 1064 nm
- Power in all non-TEM_{00} mode: less than 1 W

The laser has three frequency actuators:

- Fast: PZT of the master oscillator
- Medium: Electro Optic Modulator (EOM) (it can also be used as intensity actuator)
- Slow: Temperature control of the master oscillator (TEC)

3.2 Frequency Stabilization Servo (FSS).

The Frequency Stabilization Servo-System uses the low power beam of the laser. The frequency of the laser is compared with the reference frequency of the reference cavity using the Pound-Drever technique (Figure 4).

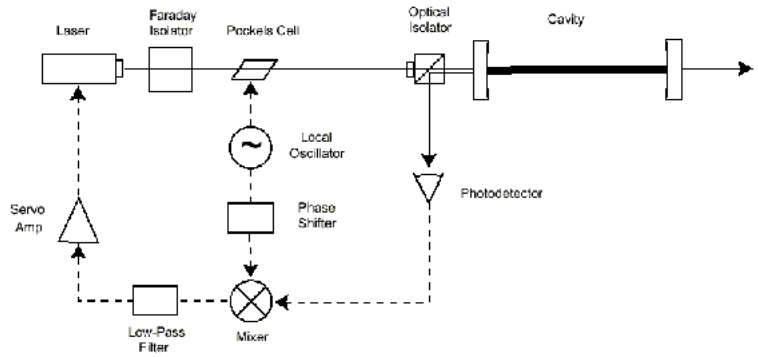

Figure 4: Pound-Drever technique.

The light can resonate in the reference cavity only if the length of the cavity is a integer number of half-wavelengths of the light. Figure 5 shows the transmission of the reference cavity as function of the frequency of the laser. The distance between two peaks is the *free-spectral range*, $f.s.r. = c/2L$, where c is the speed of light and L is the length of the cavity. The width of the peak (FWHM) is $f.s.r./F$ where F is the finesse of the cavity.

If we modulate the phase of the light at RF frequency Ω with a Pockels cell (EOM) we have actually three different beams incident on the cavity: a carrier with the same frequency of the laser ω, and two sidebands with frequency $\omega \pm \Omega$. Indeed the electric field after the EOM can be written as:

$$E_{inc} \approx E_0 e^{i(\omega t + \beta \sin \Omega t)} \approx E_0 \left[J_0(\beta) e^{i\omega t} + J_1(\beta) e^{i(\omega+\Omega)t} + J_1(\beta) e^{i(\omega-\Omega)t} \right]. \quad (6)$$

The carrier (at frequency ω) is supposed to resonate in the reference cavity (so that $\omega/2\pi = N \cdot fsr$, where N is an integer), and if it deviates from resonance, the carrier light will experience a phase shift. The sidebands (at $\omega \pm \Omega$) do not

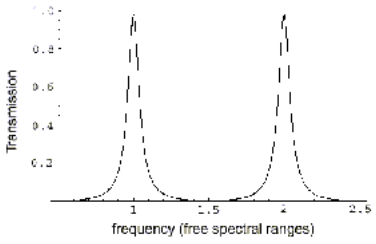

Figure 5: Transmission of the reference cavity as function of the frequency.

resonate in the cavity, so that they are promptly reflected and never experience any phase shift. The demodulation signal is proportional to the difference in phase of the carrier and sidebands, and thus to the deviation of the carrier from resonance. Figure 6 shows the FSS error signal where we can see the carrier and the sideband.

If we send this in feedback to the frequency actuators of the laser we can lock the laser frequency on the frequency of the reference cavity. In this way we reduce the frequency noise limited by the stability of the reference cavity. To have a good error signal, the reference signal must have the right phase. This phase is electronically adjusted so that there is zero output on the error signal when the carrier is fully resonant in the reference cavity. The phase shifter in Figure 4 has this goal.

To match the frequency of the laser with one resonant frequency of the cavity, there is an Acoustic Optic Modulator (AOM). After the double pass of the light through the AOM, the frequency is shifted by twice the modulation frequency of AOM. This allows additional servos (based on the 12 meter mode cleaner and the arm common mode L+ signal) to further change the laser frequency, while keeping the laser light resonant in the reference cavity.

Some parameters of the FSS are in the Table 3.2.

3.3 Pre-Mode Cleaner (PMC).

The Pre-Mode Cleaner is a triangular cavity, shown in Figure 7.

The PMC is located in the high power beam path. The light after the PMC is mainly a Gaussian TEM_{00} mode, and this decreases the intensity noise. The light resonates in the cavity only if the cavity length is an integer number of half-wavelengths. To keep the laser been resonant in the cavity, it is necessary to drive the length of the cavity with a PZT behind the concave mirror on the edge of the PMC. The error signal for the servo-system that drives the PZT is obtained with the Pound-Drever technique already explained in section 3.2. The EOM inside the MOPA applies the phase modulation. The frequency of

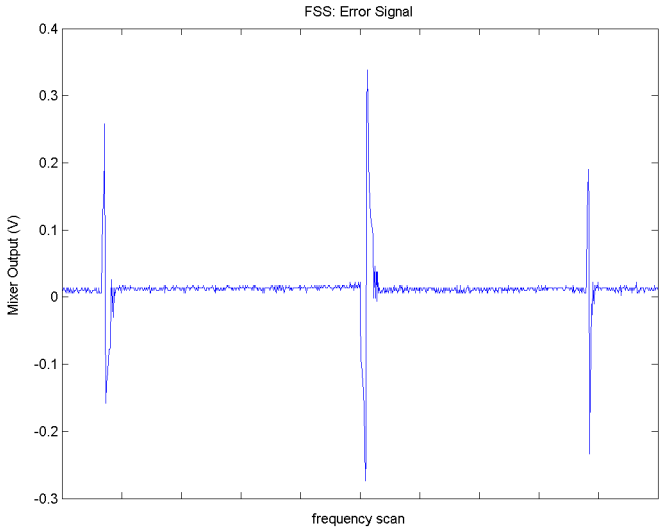

Figure 6: FSS error signal as view at the mixer output. Centered peak corresponds to resonance of the carrier, peaks to left and right correspond to the resonance of the $\omega \pm \Omega$ sidebands.

Table 1: FSS parameters.

EOM	
frequency modulation	21.5 MHz
AOM	
frequency modulation	3.3 MHz
Reference Cavity	
length	203.3 mm
free-spectral range	736.5 MHz
finesse	9518
bandwidth (FWHM)	77.4 kHz

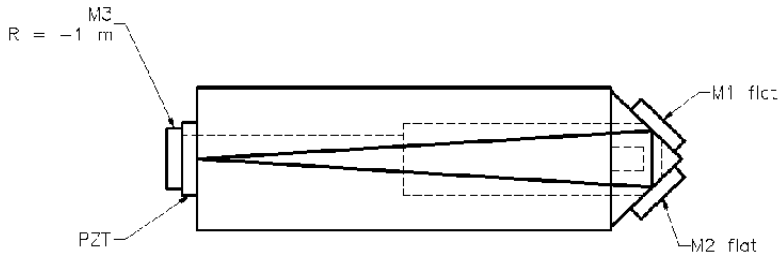

Figure 7: Pre-Mode Cleaner.

the phase modulation is 35.5 MHz. Figure 8 shows the error signal for the PMC servo-system. In Table 3.3 are reported some parameters of the PMC cavity.

Table 2: PMC parameters.

cavity length	210 mm
free-spectral range	713.8 MHz
finesse (high)	4100
bandwidth (high)	174 kHz
modulation frequency	35.5 MHz

3.4 Intensity Servo System (ISS).

The Intensity Servo System (ISS) isn't yet built in the PSL table. It is currently being designed, and there is a test prototype at Hanford.

3.5 Computer Control Interface.

All of the PSL can be controlled by computer software. With some Graphic User Interfaces (GUI) we can check the PSL parameters and change them. For example we can open or close the servo-system loops, change the gain of the loops, change the temperature of the laser, and control other many parameters. Figure 9 shows one example of these GUI: the GUI that controls the FSS.

3.6 Data Acquisition System (DAQS).

Many properties of the PSL are read from the 40m Data Acquisition System (DAQS). The DAQS uses several 32-channels Analog Digital Converters (ADCs), sampling the signals up to 2048 sample/sec. In addiction, many control and readout signals, already digitalized by the control system, are acquired

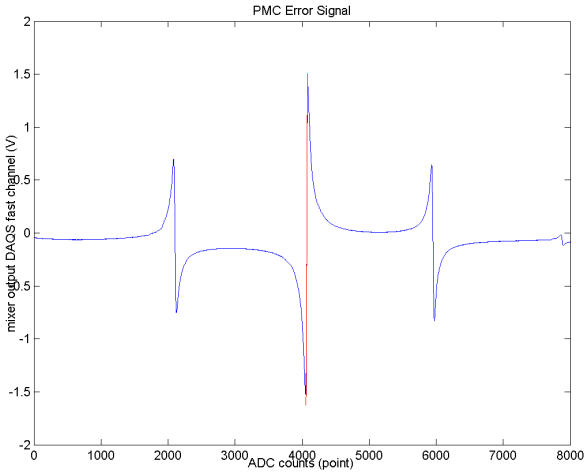

Figure 8: PMC error signal as view at the mixer output. Centered peak corresponds to resonance of the carrier, peaks to left and right correspond to the resonance of the $\omega \pm \Omega$ sidebands. The slope of the carrier has the opposite of the sign of the slope of the sidebands.

at 16 samples/sec. All the data are saved in files called *frames*. In this way we can analyze the data off-line.

4 Frequency Noise.

I measure the frequency noise when the laser is in lock with the cavity. When the laser is in lock its frequency is close to the frequency of the reference cavity and the mixer output of the FSS is proportional to the frequency shift between the laser frequency and the cavity frequency (see section 3.2). So to analyze the mixer output is the same thing to analyze the in-loop frequency noise. An independent very stable cavity is needed to better measure the true (out-of-loop) frequency noise. I analyze the data from the FSS mixer output DAQS fast channel: `PSL-FSS_MIXERM_F` .

To have the noise in the right units, it is necessary to calibrate the signal.

The calibration constant is:

$$\alpha = \frac{FWHM}{2V_{pp}^{DAQS}}. \tag{7}$$

Where V_{pp} is the voltage peak to peak of carrier in the error signal. This is true because the frequency distance between the maximum and the minimum of the error signal is equal to the FWHM of the reference cavity (77.4 kHz). There

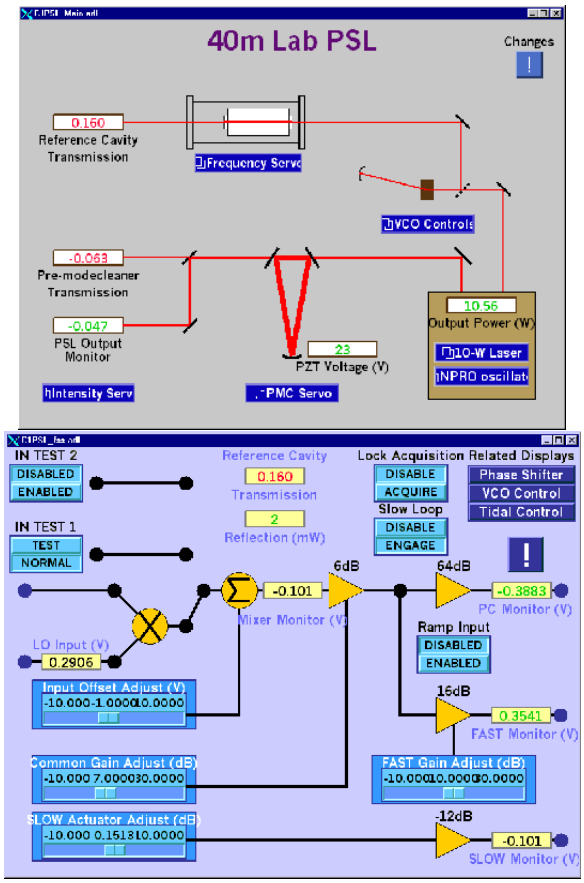

Figure 9: FSS GUIs: top-Main Laser Control GUI; bottom-FSS Control GUI.

is the factor 2 because the slope near the center of the carrier is higher. If we multiply the signal on the mixer output by α we have the frequency noise in the right unit (Hz). To see the error signal I send to the PZT laser a ramp, so the frequency of the laser changes linearly with the time. If I see how the mixer output changes in time, I see the error signal as a function of the frequency. I cannot see the entire error signal on the DAQS channel `PSL-FSS_MIXERM_F` because it saturated. So I measure V_{pp} at the output of the mixer with the scope. Figure 6 is the FSS error signal at the output of the mixer as viewed with the scope. I use that $V_{pp}^{DAQS} = V_{pp}^{scope} \cdot G$ where G is the gain of the mixer output DAQS channel `PSL-FSS_MIXERM_F` , which is known and it is equal to 100. I can obtain the frequency spectrum of the frequency noise making the Fourier analysis of the mixer output signal. Because the fast DAQS channels have sample rate of 2048pt/sec, I can make the Fourier analysis until 1kHz. I analyze the data with *Matlab*. The FFT is made using the 'Hanning' window.

Figure 10 shows two frequency noise spectra. In b) the gain is higher than in a), and the noise is lower. I cannot increase the gain too much because the loop becomes unstable. In both plots we can see peaks at odd multiples of 60 Hz. These are due to the AC power in the system. The noise is higher than the laser requirement[5] (red line in the plot) for frequency higher than 100 Hz. It's necessary to optimize all the FSS path of the light and the FSS servo-loop to improve the frequency noise.

5 PMC frequency noise.

According to section 3.3 we have to lock the length of the PMC to the wavelength of the laser. The mixer output of the PMC servo system is proportional to the frequency difference between the laser and the PMC. I can analyze this signal to find the frequency noise of the PMC. Like for the FSS frequency noise, I have to calibrate the signal. Unlike the FSS error signal, I can see the entire PMC error signal in DAQS channel: `PSL-PMC_ERR_F` . Figure 8 shows the error signal as viewed from the DAQS channel. The red line is the linear regression of the linear part of the carrier with slope s that I can calculate. I know that the distance between the two sideband Δ_{sb} corresponding in frequency to twice the modulation frequency (71 MHz). In this way the calibration constant is:

$$\alpha = \frac{71MHz}{\Delta_{sb} \cdot s}. \tag{8}$$

Figure 11 show the PMC frequency noise spectrum that is lower than the requirement [3].

6 Long Term Fluctuations.

We are interested also in the Long-Term Fluctuations of the laser. Figure 12 shows some channels of the FSS in a time period of 61 hours from August 18,2001 (GPS=682142400). The channels are from the high to the low:

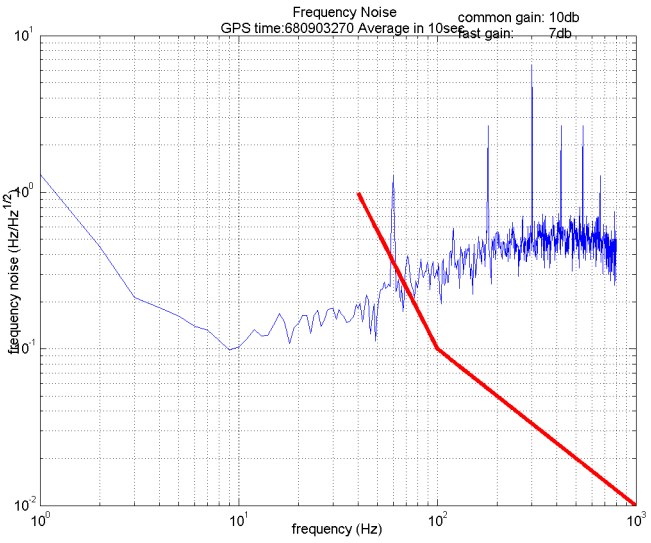

a)

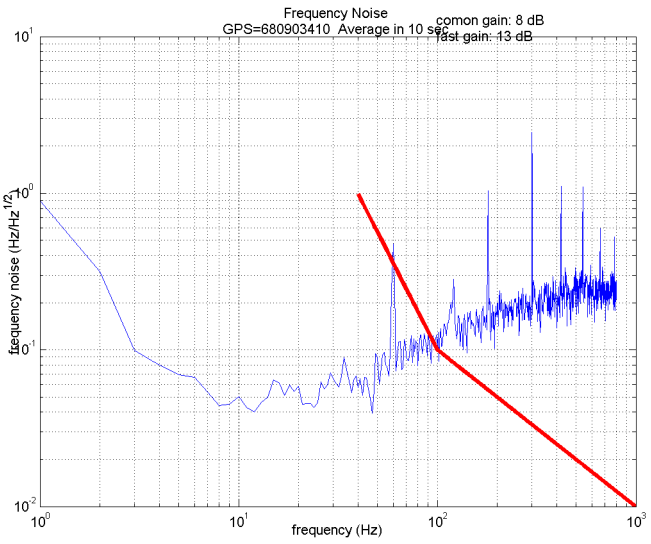

b)

Figure 10: FSS frequency noise spectrum. In b) the gain of the loop is higher than in a). The straight line is the frequency noise requirement.

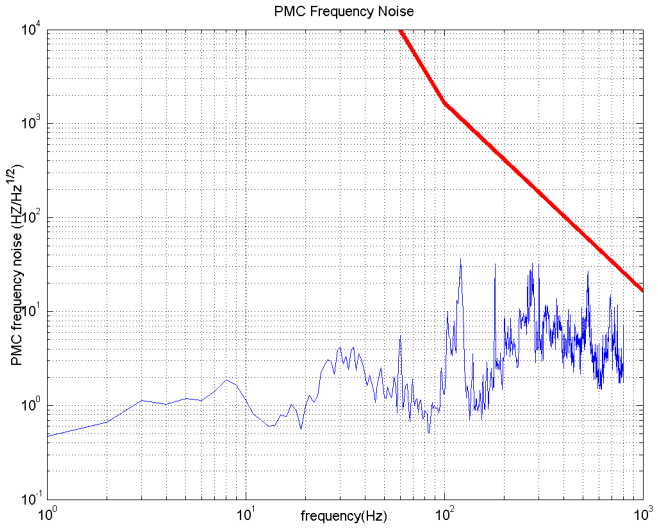

Figure 11: PMC frequency noise. The straight line is the PMC frequency noise requirement.

- `PSL-126MOPA_AMPMON:` power of the laser
- `PSL-FSS_MIXERM:` FSS mixer output
- `PSL-FSS_FAST:` FSS fast voltage monitor (PZT)
- `PSL-FSS_PCDRIVE:` FSS EOM voltage monitor
- `PSL-FSS_SLOWDC:` FSS slow actuator monitor (TEC)
- `PSL-FSS_RCTRANSPD:` FSS transmission PD
- `PSL-FSS_RFPDDC:` FSS reflected PD

Figure 13 shows some channels of the PMC in a time period of 61 hour. The channels are from the high to the low:

- `PSL-126MOPA_AMPMON:` power of the laser
- `PSL-PMC_PMCERR:` PMC mixer output
- `PSL-PMC_PZT:` PMC PZT voltage
- `PSL-PMC_PMCTRANSPD:` PMC transmission PD
- `PSL-PMC_RFPDDC:` PMC reflection PD

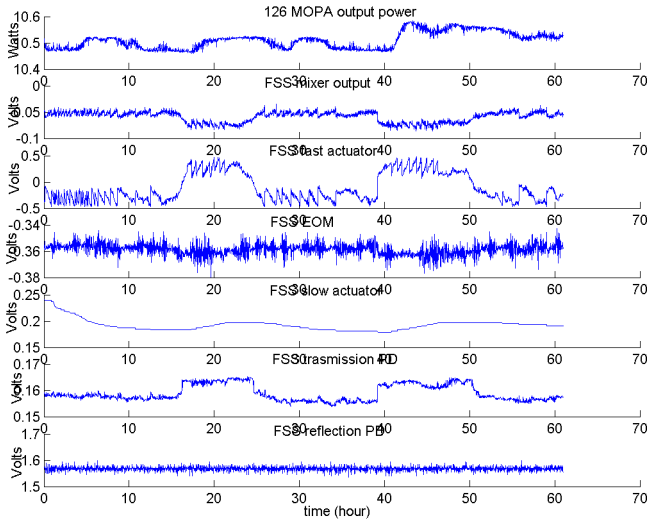

Figure 12: Long term fluctuation of the FSS channel.

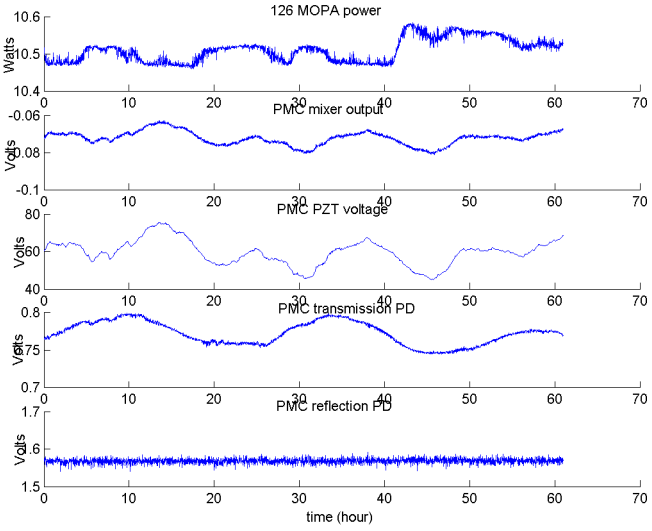

Figure 13: Long term fluctuation of the PMC channel.

Most of these signals have the same 24-hour period of oscillation. It could be due to change of temperature between the night and the day. Unfortunately, there isn't a precise temperature sensor near the PSL table to see the correlation between the temperature fluctuations and the PSL signals fluctuations.

7 Angle and Pointing Fluctuation.

We measure the angle and pointing fluctuations with Quad-Photodiodes (QPDS). The QPDS give a voltage proportional at the displacement in angle or in position of the beam. We measure the displacement on the X and Y-axis. The preliminary calibration constants are:

- position: $1mV = 30\mu m$
- angle: $1mV = 30\mu rad$

Figure 14 shows the long term fluctuation in angle and position of the beam for 61 hours. The channels in the plot are:

- `PSL-QPD1_X:` position in X axis
- `PSL-QPD1_Y:` position in Y axis
- `PSL-QPD2_X:` angle in X axis
- `PSL-QPD2_Y:` angle in Y axis

8 Intensity Noise.

We measure the power of the laser after the PMC with a photodiode (PD). First we calibrate the PD. We measure the voltage at the output of the PD at different power. Our measurements are shown in Table 8. $ScopePD$ is the voltage of the PD output viewed with the scope. $EPICSPD$ is the voltage of the PD output viewed with the DAQS slow channels `PSL-PMC_PMCTRANSPD` . $Power$ is the power of the light in front of the PD as measured with a calibrated laser calorimeter (Newport-Optical Power Meter Model 835).

Between the PMC and the PD there are two beamsplitters, so the power at the output of the PMC is not the same as the power in front of the PD. When the power in front of the PD is 1.4 mW, the power after the PMC is 1.6 mW. Figure 15 shows our measurement and the linear fit of the points. The slope is $s = 0.65$ V/mW. Figure 16 shows the power after the PMC for 61 hour. If we compare this signal with the position fluctuations along Y axis (Fig. 14) we see that they have the same shape. It is possible that the power fluctuations that we see aren't real power fluctuations but they are due to the dimension of the PD compared with the dimension of the beam. Figure 17 shows the frequency spectrum of the photodiode signal after the PMC. In this plot the signal is not calibrated.

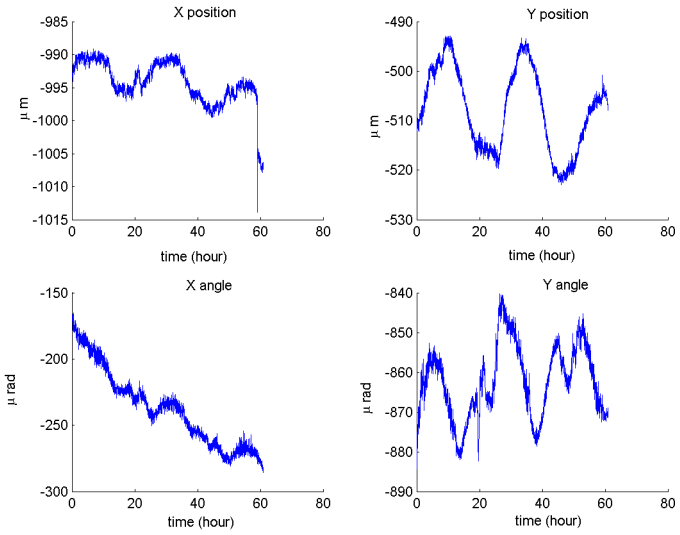

Figure 14: QPDS long term fluctuation.

Table 3: Measurement for the PD calibration.

ScopePD (V)	*EPICSPD* (V)	*Power* (mW)
-0.010	-0.067	0
1.04	0.95	1.4
2.3	2.4	3.2
3.2	3.1	4.4
4.8	4.7	6.35

9 Conclusions.

Methods for measuring many quantities characterizing the PSL performance have been developed and used, and some comparisons with the requirements have been made. Further work is required to improve the laser performance, guided by these results.

Acknowledgments.

I want to thank all the people that work in the caltech 40m laboratory: Alan Weinstein, Dennis Ugolini, Steve Vass, Ben Abbott and all the other 40m SURF students: Irena, Mihail, Richard, Tim, Victor. I also want to thank Francesco Fidecaro and Rosalia Stellacci.

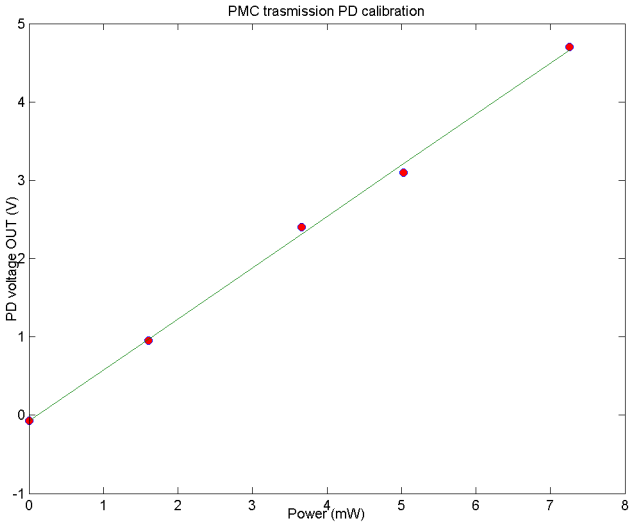

Figure 15: Photodiode voltage in function of the power after the PMC.

References

[1] P.R. Saulson, *Fundamentals of Interferometric Gravitational-wave Detectors* (World Scientific, 1994).

[2] *(Infrared) Pre-stabilized Laser (PSL) Conceptual Design* **LIGO-T970087-04-D**.

[3] *(Infrared) Pre-stabilized Laser (PSL) Final Design* **LIGO-T990025-00-D**.

[4] *An Introduction to Pound-Drever-Hall Laser Frequency* **LIGO-P990042-00-D**.

[5] *LIGO Hanford Observatory 2k IFO PSL Test Report* **LIGO-T000031-00-D**.

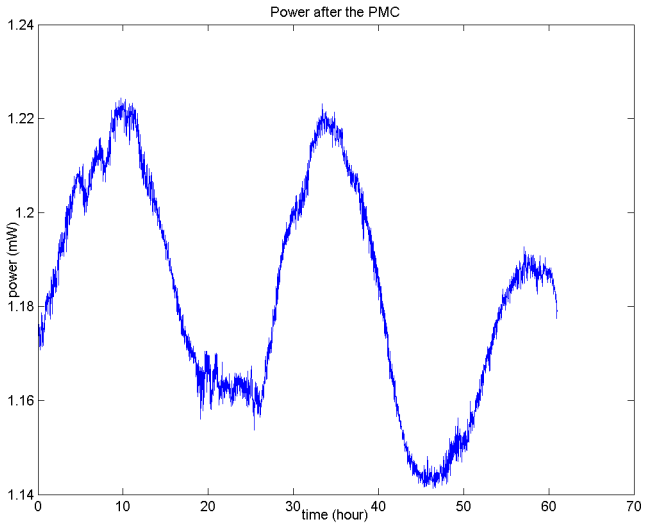

Figure 16: power of the laser after the PMC

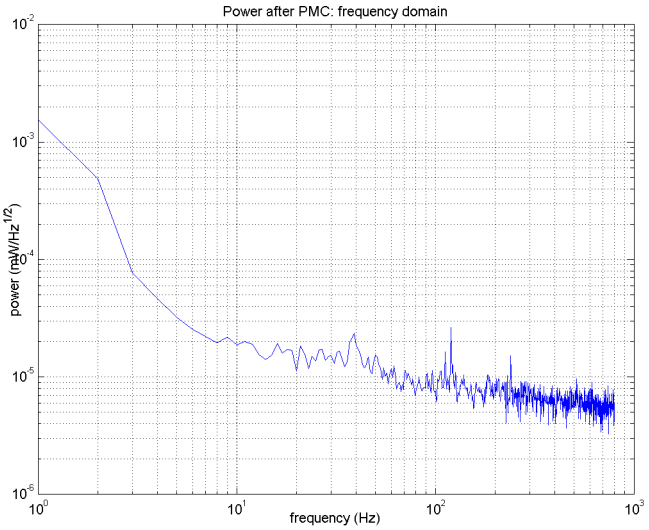

Figure 17: PMC transmission power noise.